Original Article

MOLECULAR METABOLISM

Glycolysis maintains AMPK activation in sorafenib-induced Warburg effect

Sijia Guo [1,5], Chenhao Zhang [1,5], Haiou Zeng [2], Yantao Xia [3], Chenghao Weng [1], Yichen Deng [1], Luda Wang [2], Huan Wang [1,*,4]

ABSTRACT

Hepatocellular carcinoma (HCC) is the second deadly cancer in the world and still lacks curative treatment. Aerobic glycolysis, or Warburg effect, is a major resistance mechanism induced by first-line treatment of HCC, sorafenib, and is regulated by the master regulator of metabolism, AMPK. Activation of AMPK is required for resistance; however, activation dynamics of AMPK and its regulation is rarely studied. Engineering cells to express an AMPK activity biosensor, we monitor AMPK activation in single HCC cells in a high throughput manner during sorafenib-induced drug resistance. Sorafenib induces transient activation of AMPK, duration of which is dependent on glucose. Inhibiting glycolysis shortens AMPK activation; whereas increasing glycolysis increases its activation duration. Our data highlight that activation duration of AMPK is important for cancer evasion of therapeutic treatment and glycolysis is a key regulator of activation duration of AMPK.

Keywords AMPK; Hepatocellular carcinoma; Glycolysis; Drug sensitivity; Sorafenib

1. INTRODUCTION

AMP-activated protein kinase (AMPK) is a heterotrimeric protein kinase and functions as a sensor and guardian of energy homeostasis [1]. Upon energy deficiency in forms of nutrient or oxygen deprivation, cellular AMP/ADP:ATP ratio increases and the accumulated AMP activates AMPK through binding with its γ subunit to elicit conformational changes that facilitate phosphorylation at threonine 172 and decrease its dephosphorylation. Besides sensing adenine nucleotide levels, AMPK senses the absence of glucose [2,3], or an increase in intracellular calcium [4–6] and is also post-translationally regulated by other pathways, such as AKT or S6K, reactive oxygen species and ubiquitination [1]. Once AMPK is activated, it phosphorylates up to 100 substrates to promote catabolism and inhibit anabolism in order to restore energy homeostasis. It remains unclear how AMPK coordinately regulates so many substrates and pathways.

Spatial and temporal regulation of AMPK diversifies its function [7]. Spatially, AMPK is acutely activated on lysosome by the vATPase-Regulator-adolase-AXIN-LKB1 complex upon glucose depletion [8]. High or moderate elevations of AMP activate AMPK on mitochondria or in cytoplasm respectively [9]. In response to cardiac ischemia/reperfusion, γ2-AMPK translocates into the nucleus and suppresses pre-rDNA transcription and ER stress to reduce infarct size [10]. So, different signals elicit compartmentalization of AMPK to allow selective regulation of its targets. Compared with spatial regulation, temporal modulation of AMPK has been less studied. During hypoxia, AMPK activity increases at 1 ~ 2 h, decreases at 4 ~ 8 h, and peaks at 15 h in H9C2 cells [11]. CCCP, a mitochondrial uncoupler, causes acute AMPK activation after 2 min to phosphorylate ULK1, which then activates Parkin and mitophagy [12]. AMPK is required for the inhibition of mTORC1 by oligomycin at the early stage (0 ~ 1 h), but not at the later stage [13]. It is speculated that acute effects of AMPK are to revert energy deficiency and chronic effects modulate transcription or organelle biogenesis/recycling [7,12]. To better understand the temporal role of AMPK on regulating energy homeostasis, it is worthwhile to measure its activation dynamics more accurately.

AMPK activity reporter (AMPKAR) is built to enable real-time monitoring of temporal and spatial changes of AMPK in living cells [14]. In energy deficiency, AMPK is activated in subcellular regions with different kinetics, with the fastest activation in cytoplasm [15]. Recently, a single-fluorophore AMPKAR (ExRai AMPKAR) was developed and used to discover nuclear AMPK activity and spatial regulation of AMPK by upstream kinases [16]. AMPK also showed steady or oscillatory forms of activation in response to different metabolic perturbations [17]. When AMPKAR was used to monitor the AMPK activity *in vivo,* it elucidated tissue-specific activation of AMPK such that metformin activates AMPK in the liver and AICAR in the skeletal muscle [18]. AMPKAR measures the dynamic changes of AMPK in response to energy stresses, providing new insights for the understanding of AMPK

[1]Institute of Systems Biomedicine, Beijing Key Laboratory of Tumor Systems Biology, School of Basic Medical Sciences, Peking University Health Science Center, Beijing, 100191, China [2]National Key Laboratory of Science and Technology on Micro/Nano Fabrication, School of Integrated Circuit, Peking University, Beijing, 100871, China [3]University of California Los Angeles, Department of Chemical and Biomolecular Engineering, California, 90095, USA

[4] Lead Contact.
[5] these authors contributed equally to the work.

*Corresponding author. No.38 Xueyuan Road, Peking University Health Science Center, Beijing, 100191, China. E-mail: huan_sharon_wang@pku.edu.cn (H. Wang).

Received March 28, 2023 • Revision received August 19, 2023 • Accepted August 29, 2023 • Available online 9 September 2023

https://doi.org/10.1016/j.molmet.2023.101796

regulation on energy homeostasis as well as pharmacology of drugs that modulate AMPK.

AMPK is a drug target for treating type II diabetes, obesity and cancer [19]. Sorafenib (NEXAVAR®, BAY43-9006) is a small molecule multi-kinase inhibitor approved as first-line treatment for advanced renal cell carcinoma, hepatocellular carcinoma (HCC) and thyroid cancer. However, therapeutic effect of sorafenib is often overcome by primary or acquired drug resistance, one of which is "Warburg effect", or aerobic glycolysis [20]. Inhibiting aerobic glycolysis through HK2 [21], PFKFB3 [22], PDK1 [23] inhibition or fasting [24] acts synergistically with sorafenib to kill HCCs. AMPK is essential in regulating resistance in HCCs such that AMPKα knockdown increases cell death in response to sorafenib and a glycolysis inhibitor and AMPK also up-regulates glycolysis [25]. Despite the important role of AMPK in sorafenib-induced Warburg effect, the dynamics of AMPK activity during this therapy remains unclear. To answer this question, we established hepatocellular carcinoma cells with AMPKAR to measure AMPK dynamics at the single-cell level. Elucidation of this could facilitate the understanding of drug resistance origination and maintenance in sorafenib treatment.

2. MATERIALS AND METHODS

2.1. Huh7 general culture

Cells were cultured in growth medium (DMEM+10% FBS) to reach logarithmic growth stage and were harvested to seed at specified density in different plates. Cells were then cultured for 24 h in a 37 °C,5% CO_2 incubator. After pre-culture, medium was exchanged to DMEM without FBS to synchronize cells for 14 h. Then, media with different glucose concentrations were replaced 1 or 2 h before drug treatment. All DMEM media contain 1 mM pyruvate and 4 mM L-glutamine.

2.2. Generation of Huh7 cells with AMPKAR2 biosensor

Cells were seeded onto 6-well plates at a density of 2.5×10^5 cells/well and cultured in a 37 °C,5% CO_2 incubator. When cells reached 60–80% confluency, they were co-transfected with the pPBJ-puro-AMPKAR2-nes and the pCMV-hyPBase plasmids at a ratio of 2:1 using jetPRIME transfection reagent according to the manufacturer's instructions. 48 h after transfection, Huh7 cells with stable expression of AMPKAR2 were selected with puromycin at concentrations of 1.0–4.0 μg/mL for 12–14 days. Then, cells with high expression of AMPKAR2 were sorted by fluorescence activated cell sorting and grown from single sorted cells.

2.3. High content imaging

Huh7 cells expressing AMPKAR2 were imaged using the ImageXpress Micro Confocal High Content Imaging System (Molecular Devices). Cells were seeded into a 24-well glass bottom plate at a density of 9×10^4/well and cultured as in "Huh7 general culture". One hour before shooting, medium was replaced with DMEM (without FBS, without phenol red, with HEPES) with different glucose concentrations after washing once with 1× PBS solution. During imaging, cells were placed in a 37 °C, 5% CO_2 environment. After about 1 h of baseline imaging, different drugs were added using a 4× or 5xconcentrated concentration. Sorafenib was treated at 10 μM, so it was prepared as a 50 μM (5×) stock before adding to cells. DMSO level was limited to be ≤0.2%. For dual drug stimulation, second drug was added at a 4× or 5× concentration after three images had been acquired since the first drug addition. To obtain fluorescence from both mTurquoise2 (cyan fluorescence protein, CFP) and YPet (yellow fluorescence protein, YFP) channels, blue light filtered by 438/29 nm was used to excite cells, and light emitted around 483/32 nm and 562/40 nm was collected. Images were acquired every 6 min except after each drug addition, which took 15～30 min. Compound C was treated at 10 μM, 2-DG at 25 or 100 mM, glucose at 12.5 or 25 mM.

2.4. Image analysis

Images were imported to Fiji as an image sequence. Fiji plugin TrackMate-Cellpose was used to detect single cell masks and track cell trajectories in the image sequences. A pre-trained neural network model based on the cellpose algorithm was used to identify the cytoplasm of cells. Initial guess for cell diameter, a cellpose model parameter, was set to 30 pixels. All the spots converted from cell masks were reserved for subsequent analysis. Linear assignment problem (LAP) Tracker was selected to track cell trajectories. Other parameters were set as default. The cytoplasm after excluding the nucleus was selected as the region of interest (ROI) for each cell, and fluorescent intensity of ROIs were calculated by customized matlab scripts (https://github.com/xyttyxy/bjmu). Average fluorescence intensity of mTurquoise2 (CFP) or YPet (YFP) in regions of interest (ROIs) at every time point was calculated, and background fluorescence intensity at the corresponding time points of each channel was subtracted. AMPK index was calculated as follows: ratios of mTurquoise2 to YPet were calculated and multiplied by −1. This value was added by 1 to set most values to be positive numbers in each experiment. For most experiments, manual selection of 30～100 ROIs in different cells was performed and the results were consistent with the automatic analysis (data not shown). For FRET ratio analysis in Figure 1B, images were background corrected and fluorescence intensity of YPet or mTurquoise2 in the cytoplasm was quantified. The ratio of fluorescence intensity between YPet and mTurquiose2 was calculated and used accordingly to pseudo-color single cells.

2.5. Activation duration of AMPK analysis

Activation duration of AMPK was analyzed by MATLAB (MathWorks, R2019b) based on AMPK index derived from analyzing fluorescence ratios that correlates with AMPK activity. In these curves, continuous decreases occur after a sudden rise of index, and the decline rate slows down gradually. Deactivation point of AMPK is defined as the starting point of a continuous decrease in AMPK index. Slopes between each adjacent time point of AMPK index were calculated. Positive slopes were set to 0, while negative slopes unchanged. Then, the time point where the slope value changed most is the deactivation point of AMPK. Additionally, for the curves that have a slight decline followed by an increase, we rule out this "dip" region by analyzing whether there is a significant increase after the time point, and then we take this point as the starting point to find the time where the slope value changed most again. Activation duration of AMPK equals to the time difference between the deactivation points and time 0. For the curves that fluctuate without a continuous decline, activation duration of AMPK is set to the maximum time of imaging.

2.6. CCK8 assay

Cells were seeded evenly into 96-well plates at a density of 1.2×10^4/well and cultured as in "Huh7 general culture". Edge wells were sealed with 100 μL/well of 1 × PBS solution. Media with different glucose concentrations (0～25 mM) were replaced 2 h before drug treatment. After treating with different combinations of drugs (sorafenib, compound C, 2-DG, glucose) for designated times, 10 μL CCK-8 reagent (TargetMol) was added to each well. Plates were incubated for 2 h and absorbance at 450 nm was measured by a FlexStataion 3 microplate reader.

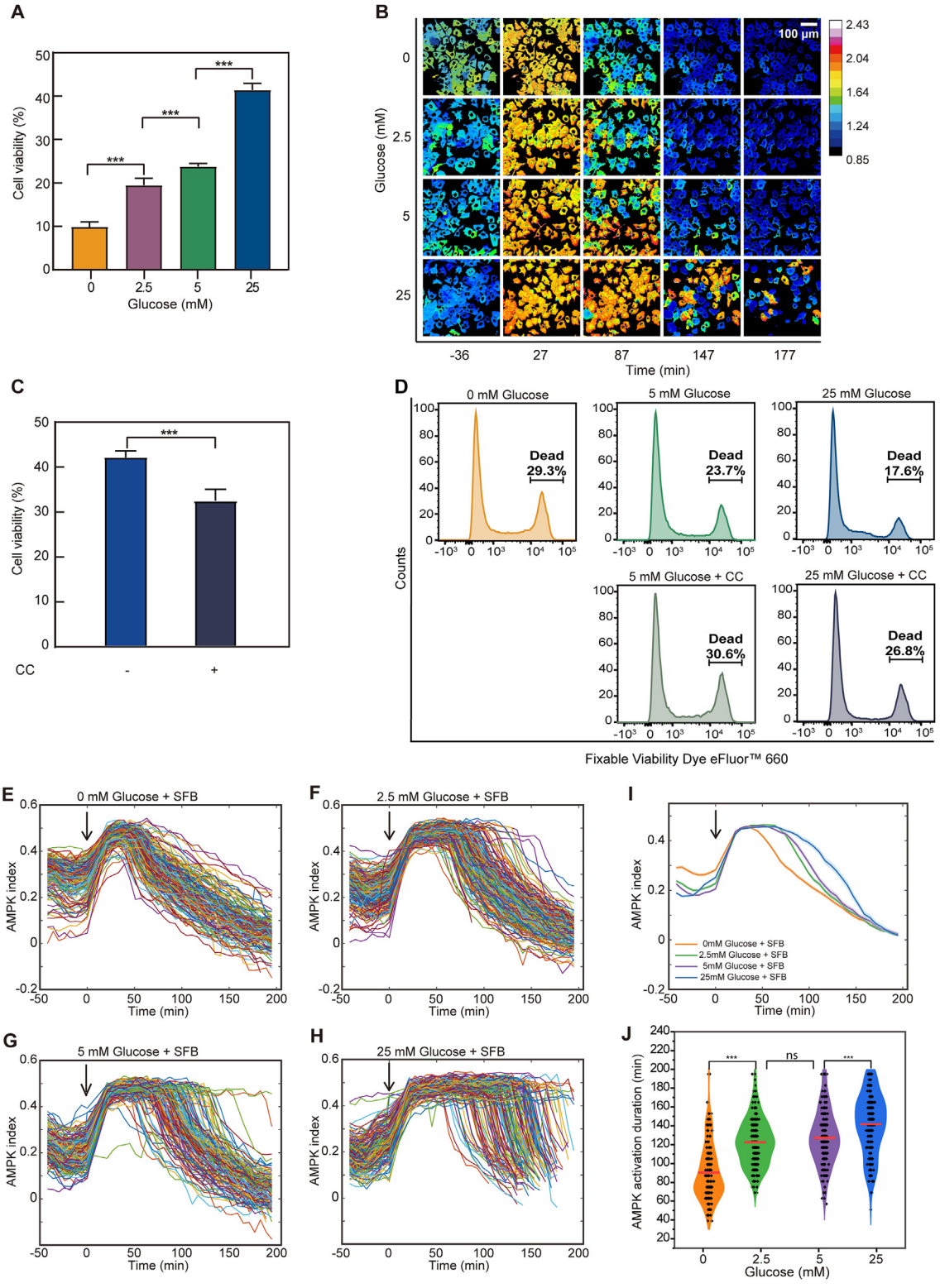

Figure 1: Glucose extends activation duration of AMPK in response to sorafenib. (A) Viability of Huh7-AMPKAR2 cells treated with sorafenib (SFB, 10 μM) in different glucose concentration for 3 h. (B) FRET signal of AMPKAR2 was calculated by the ratio of fluorescence intensity of YPet to mTurquoise2, color-coded and projected onto cells treated with SFB (10 μM) in different glucose cultures. (C) Viability of Huh7-AMPKAR2 cells cultured in high glucose and treated with sorafenib ± compound C (both at 10 μM). (D) Percent of dead cells in response to sorafenib ± compound C in different glucose concentration measured by flow cytometry. (E–H) Single cell traces of AMPK index in Huh7-AMPKAR2 cells treated with sorafenib and cultured at 0, 2.5, 5 and 25 mM of glucose. (I) Mean (solid line) and 95% confidence interval (shades) for traces of AMPK index from (E–H). Arrow: time point of sorafenib addition. (J) Activation duration of AMPK to sorafenib at different glucose concentrations. ***$p < 0.001$. Data representative of three independent experiments.

2.7. Seahorse assay

Cells were seeded evenly into Seahorse XF96 cell culture plates (Agilent) at a density of 6.25×10^3 cells/well and cultured as in "Huh7 general culture". About 2 h before the test, cells were moved to a non-CO_2 incubator at 37 °C and incubated for 1 h 1 h prior to the test, cell suspension was replaced with the Seahorse Basal DMEM at 37 °C (with appropriate concentration of glucose, 4 mM L-glutamine, 1 mM sodium pyruvate and 1% penicillin-streptomycin solution) and incubated in a non-CO_2 incubator at 37 °C for 1 h. Drugs were prepared at 8× to 10× concentrations with the corresponding media as in each well and added into ports of Seahorse XF96 cartridge plates which have been hydrated overnight. XFe96 Extracellular Flux Analyzer (Agilent) was used to measure oxygen consumption rate and extracellular acidification rate of cells with different drug treatments.

2.8. Metabolomics

Huh7-AMPKAR2 cells cultured in high glucose (25 mM) and treated with DMSO or sorafenib and subsequently treated with or without 25 mM 2-DG were collected by lysing in 80% methanol (HPLC-grade, pre-chilled at −80 °C). Similarly, cells cultured in low glucose (2.5 mM) and treated with DMSO or sorafenib and subsequently treated with or without 22.5 mM glucose were collected. Samples were incubated in −80 °C overnight and centrifuged at 14,000 g for 20 min at 4 °C. Supernatant was transferred into a fresh tube. Samples were dried using a speedvac at room temperature and sent immediately to the facility for metabolomics quantification.

Targeted metabolomics, focused on TCA cycle, glycolysis pathway, pentose phosphate pathway, amino acids and purine metabolism, was analyzed by TSQ Quantiva (Thermo, CA). C18-based reverse phase chromatography was done with 10 mM tributylamine, 15 mM acetate in water and 100% methanol as mobile phase A and B respectively. A 25-minute gradient from 5% to 90% mobile B was used. Positive-negative ion switching mode was performed for data acquisition. The resolution for Q1 and Q3 are both 0.7FWHM. The source voltage was 3500v for positive and 2500v for negative ion mode. The source parameters are as follows: spray voltage: 3000v; capillary temperature: 320 °C; heater temperature: 300 °C; sheath gas flow rate: 35; auxiliary gas flow rate: 10. Metabolite identification was done based on Tracefinder search with a home-built database containing about 300 compounds.

2.9. Western blot

Cells were seeded onto 6-well plates at a density of 3.5×10^5 cells/well and cultured as in "Huh7 general culture". After drug treatment, media was removed and cells were washed once with cold 1xPBS. Cells were lysed on ice for 30 min with the RIPA buffer with protease and phosphatase inhibitors. Cells were scraped off the plate and centrifuged at 12,000 RPM for 20 min at 4 °C. Supernatant was transferred into new tubes and protein concentration was determined by the BCA method. Proteins were heated at 95∼100 °C for 5 min and 16∼24 μg total protein was loaded onto a polyacrylamide gel at 7.5−10%. After electrophoresis and wet transfer, PVDF membranes were blocked by 5% non-fat milk or 3% BSA (bovine serum albumin) in TBST for 2 h at room temperature. Then, blots were incubated with a primary antibody diluted at 1:1000 (except β-actin at 1:20000) in TBST with 1.5% BSA overnight at 4 °C. After TBST wash for 3 times, blots were incubated with the corresponding secondary antibodies and visualization through enhanced chemiluminescence and X-ray films. Gray values of bands were quantified using ImageJ.

2.10. Flow cytometry

Drug-treated Huh-7-AMPKAR2 cells were washed with 1xPBS twice, dissociated by accutase treatment and stained with eBioscience™ Fixable Viability Dye eFluor™ 660 at 1:1000 in PBS following the manufacturer's protocol. After incubation at 4 °C for 30 min, cells were washed with PBS once and re-suspended in PBS. Cells were filtered through a 40 μm strainer and analyzed by a flow cytometer immediately.

3. RESULTS

3.1. Activation duration of AMPK is longer in high glucose-induced resistance to sorafenib treatment

To monitor AMPK activity and study its role in drug resistance in single HCCs in real time, we generated Huh7 cells that stably express a fluorescence resonance energy transfer (FRET)-based biosensor, AMPKAR2 [17] (see also Figure. S1A), termed Huh7-AMPKAR2 cells. Consistent with previous studies [23], Huh7-AMPKAR2 cells showed higher level of drug resistance to sorafenib in high glucose as cell viability was increased by 2∼4 folds in high glucose (25 mM) than in no or low glucose (0 or 2.5 mM, Figure 1A). In addition, the fraction of dead cells induced by sorafenib was increased from 18% in 25 mM glucose to 29% in 0 mM glucose, indicating higher drug resistance in high glucose culture (Figure 1D). To evaluate the dynamics of AMPK in this sorafenib-resistant cell model, we measured AMPK activity in live Huh7-AMPKAR2 cells via FRET-based high content imaging. We observed that sorafenib induced transient activation of AMPK at any glucose concentration, however the dynamics of AMPK activity varied among treatments and cells (Figure 1B). Cells cultured at 25 mM glucose had the longest activation duration of AMPK in a heterogeneous manner (Figure 1B). To validate that AMPK plays an important role in Huh7's resistance to sorafenib at high glucose, we used compound C to inhibit AMPK activity. Compound C treatment caused a decrease in cell viability (from ∼40% to 30%, Figure 1C), and an increase in cell death (from 18% to 27% in 25 mM glucose culture, and from 24% to 31% in 5 mM glucose culture, Figure 1D), indicating the importance of AMPK in maintaining cell viability and in preventing cell death in response to sorafenib.

To test whether the dynamics of AMPK activity has a correlation with the glucose-dependent drug resistance, we segmented and traced 200 to 400 single cells automatically over 3∼4 h of drug treatments, and analyzed the fluorescent intensities of CFP and YFP encoded by AMPKAR2. AMPK index correlates better with the percentage of activated AMPK than the FRET ratio [17], so it was used as a surrogate measurement of AMPK activity. Sorafenib induced an acute increase in the AMPK index right after administration, and maintained AMPK index for different duration in different glucose cultures (Figure 1E-I). Activation duration of AMPK, defined by the time span between the initial rise and when AMPK indexes fall to the baseline levels, was increased in a glucose-dependent manner (Figure 1I,J). Activation duration of AMPK to sorafenib was 90.4, 122.6, 127.4 and 141.9 min in average at 0, 2.5, 5 and 25 mM glucose and the differences were significant between high and medium or medium and no glucose conditions (Figure 1J). To validate that Huh7-AMPKAR2 cells respond to AMPK activation, we treated cells with an AMPK activator, A769662, or a glycolysis inhibitor, Iodoacetate, as positive controls. AMPK index was increased to a similar level by these two drugs (Figures. S1B−S1D) and ACC phosphorylation, which is a gold standard for measuring AMPK activity, was also increased to a similar level by these treatments (Figure. S1E). To rule out that AMPK deactivation is a result of cell death, we quantified cell death based on entry of fluorescence into

nuclei (as the AMPKAR2 sensor has a nucleus exclusion signal and it is normally expressed in cytoplasm). Reduction of the AMPK index proceeded the re-localization of AMPKAR2 to nuclei or cell death by many time points, indicating that deactivation happened before cell death (Figure. S2). Therefore, activation duration of AMPK in response to sorafenib increases with glucose concentration and correlates with higher cell viability or drug resistance.

To validate the inhibitory effect of sorafenib on mitochondrial respiration, we examined the oxygen consumption by seahorse experiments. About half an hour after sorafenib treatment, oxygen consumption rate (OCR) was decreased to a similar extent from 93.3 $\pm$ 13.5 pmol/min to 35.6 $\pm$ 8.2 pmol/min in no glucose and from 97.6 $\pm$ 10.1 to 40.5 $\pm$ 7.7 in 25 mM glucose (Figure. S3A). This suggests that sorafenib inhibits mitochondrial respiration similarly at different glucose concentrations. To confirm that cells in high glucose culture consumed more glucose, we measured extracellular acidification rate (ECAR) of Huh7-AMPKAR2 cells cultured in no or high glucose. ECAR was increased from 16.5 $\pm$ 2.7 mpH/min in no glucose to 27.0 $\pm$ 1.8 mpH/min in high glucose, indicating that cells metabolized more glucose into lactate in the later condition (Figures. S3C and S3D). As solvent for sorafenib, DMSO (dimethyl sulfoxide) was added at the same amount and the same time as sorafenib as a negative control. AMPK index did not change in response to DMSO at any glucose concentration, supporting that the changes in AMPK index induced by sorafenib was not due to the blank solvent (Figures. S3E—S3I). Basal AMPK index was higher in no glucose than in the higher glucose concentrations (Figure. S3I), consistent with AMPK activation in response to glucose depletion and the result in Figure 1I.

3.2. Glycolysis is necessary for maintaining AMPK activation in response to sorafenib in high glucose

As higher glucose concentration and glycolysis correlate with longer AMPK activation induced by sorafenib, we asked whether glycolysis is necessary for maintaining AMPK activation. To test whether glycolysis is necessary for maintaining AMPK activation, we used 2-deoxyglucose (2-DG), a competitive inhibitor of hexokinase II that catalyzes the first step in glycolysis. As the high glucose media contain 25 mM glucose, we chose 2-DG at the same or 4-fold concentration of glucose to inhibit glycolysis. To test whether 2-DG inhibits glycolysis at the selected dose, we measured ECAR when cells were treated with DMSO/sorafenib and 2-DG sequentially in high glucose. In both DMSO- and sorafenib-treated condition, 2-DG acutely inhibited ECAR, but not OCR, as soon as 6 min after stimulation (Fig 2B,A). When glycolysis was inhibited by 2-DG (25 or 100 mM) after sorafenib pretreatment, activation duration of AMPK was significantly shortened (Figure 2G) and nearly no cell had sustained activation for the entire imaging period compared with the control (Figure 2C,D & 2E). The inhibitory effect of 100 mM 2-DG on activation duration of AMPK was slightly stronger than 25 mM 2-DG (Figure 2F,G). In controls with sequential treatment of DMSO and 2-DG, AMPK index was not affected by DMSO, but elevated by 2-DG (25 or 100 mM) (Figures. S4A—S4C). This is as expected, as 2-DG inhibits ATP generation from glycolysis and activates AMPK, and suggests that the inhibition of AMPK by 2DG under sorafenib treatment is not due to 2DG alone. Since high concentration of 2-DG causes other off-target effects, such as ER stress and changes in calcium [26,27], we tested another inhibitor of glycolysis, 3-(3-pyridinyl)-1-(4-pyridinyl)-2-propen-1-one (3PO), which inhibits PFKFB3 [28]. Consistent with the effects of 2-DG, 3PO shortened activation duration of AMPK after sorafenib pretreatment (Figure. S6). These results collectively show that glycolysis is required for maintaining AMPK activation under sorafenib treatment in high glucose.

To support the results of FRET experiments, western blot was used to measure ACC phosphorylation as a readout of AMPK activity. Similar to the increases in AMPK index after sorafenib treatment in the FRET experiments, ACC phosphorylation was increased by sorafenib at 15 min and 2 h (Figure 2I). When 2-DG was added after DMSO, it increased AMPK activity similarly as in the FRET experiments (Figure 2I & S4). When 2-DG was added 30 min after sorafenib, the combination inhibited ACC phosphorylation compared with sorafenib alone (Figure 2I,J). This is also consistent with the findings in FRET that 2-DG shortened AMPK activation (Figure 2G). 2-DG in combination with sorafenib also decreased cell viability (Figure 2H), indicating the crucial role of glycolysis in maintaining viability in response to sorafenib.

Since AMPK activity is regulated by AMP or ADP to ATP ratios, we measured the levels of these adenine nucleotides in different drug treatments and found that the AMP/ATP or ADP/ATP ratio was increased when sorafenib was supplemented (Figures. S4E—S4G). The AMP/ATP ratio was further increased by the combination of sorafenib and 2-DG, compared with sorafenib alone (Figure. S7B), which would increase AMPK activity. However, AMPK activity was inhibited by the combination of sorafenib and 2-DG than sorafenib alone as measured in FRET or western blots, so this cannot be caused by the AMP/ATP ratio. This indicates that factors other than adenine nucleotides are responsible for how glycolysis regulates AMPK dynamics under sorafenib treatment.

3.3. Glycolysis is sufficient for maintaining AMPK activation in response to sorafenib in low glucose

To test whether glycolysis is sufficient to maintain AMPK activation under sorafenib treatment, we supplemented glucose to the final concentrations of 12.5 or 25 mM in no or low glucose (0 or 2.5 mM glucose) culture. When glucose was added to cells cultured in no glucose at about 30 min after DMSO or sorafenib, ECAR was increased from 16.7 $\pm$ 2.0 to 26.4 $\pm$ 2.3 and 14.2 $\pm$ 3.3 to 22.9 $\pm$ 5.6 respectively, but OCR was not changed significantly (Figure 3A,B). This suggests that glucose supplementation increases glycolysis metabolism into lactate. When Huh7-AMPKAR2 cells were cultured in low glucose (2.5 mM) and treated with sorafenib, very few cells (3.6%) had persistent AMPK activation over the duration of imaging ($\sim$200 min in total, Figure 3C). However, glucose supplementation to 12.5 mM or to 25 mM caused 45.0% or 71.0% of cells to have persistent AMPK activation over the duration of imaging (Figure 3D,E). The average activation duration of AMPK after sorafenib treatment was 91.1, 159.8 and 180.6 min in cells cultured in low glucose, glucose supplemented to 12.5 mM or to 25 mM (Figure 3G). 25 mM glucose supplementation extended the average activation duration of AMPK longer than 12.5 mM (Figure 3F,G). Similarly, when Huh7-AMPKAR2 cells were cultured in no glucose and glucose was supplemented about 30 min after sorafenib treatment, AMPK activation was also extended. 39.6% of cells in 12.5 mM glucose and 57.6% cells in 25 mM glucose had persistent AMPK activation over the duration of imaging ($\sim$223 min, Figure S5A-S5C, S5G, S5H). For Huh7-AMPKAR2 cells cultured in no or low glucose and treated with DMSO, AMPK activity was reduced by glucose supplementation (Figures. S5D—S5F, S5I—S5M). This is as expected, as glucose supplementation may increase ATP generation from glycolysis and inhibit AMPK, and suggests that the maintenance of the AMPK activity by glucose supplementation during sorafenib treatment was not due to glucose alone. In summary, we find that increasing glucose and its metabolism to lactate drive persistent AMPK activation under sorafenib treatment.

To validate the results obtained by FRET, we measured ACC phosphorylation levels by western blots. ACC phosphorylation was

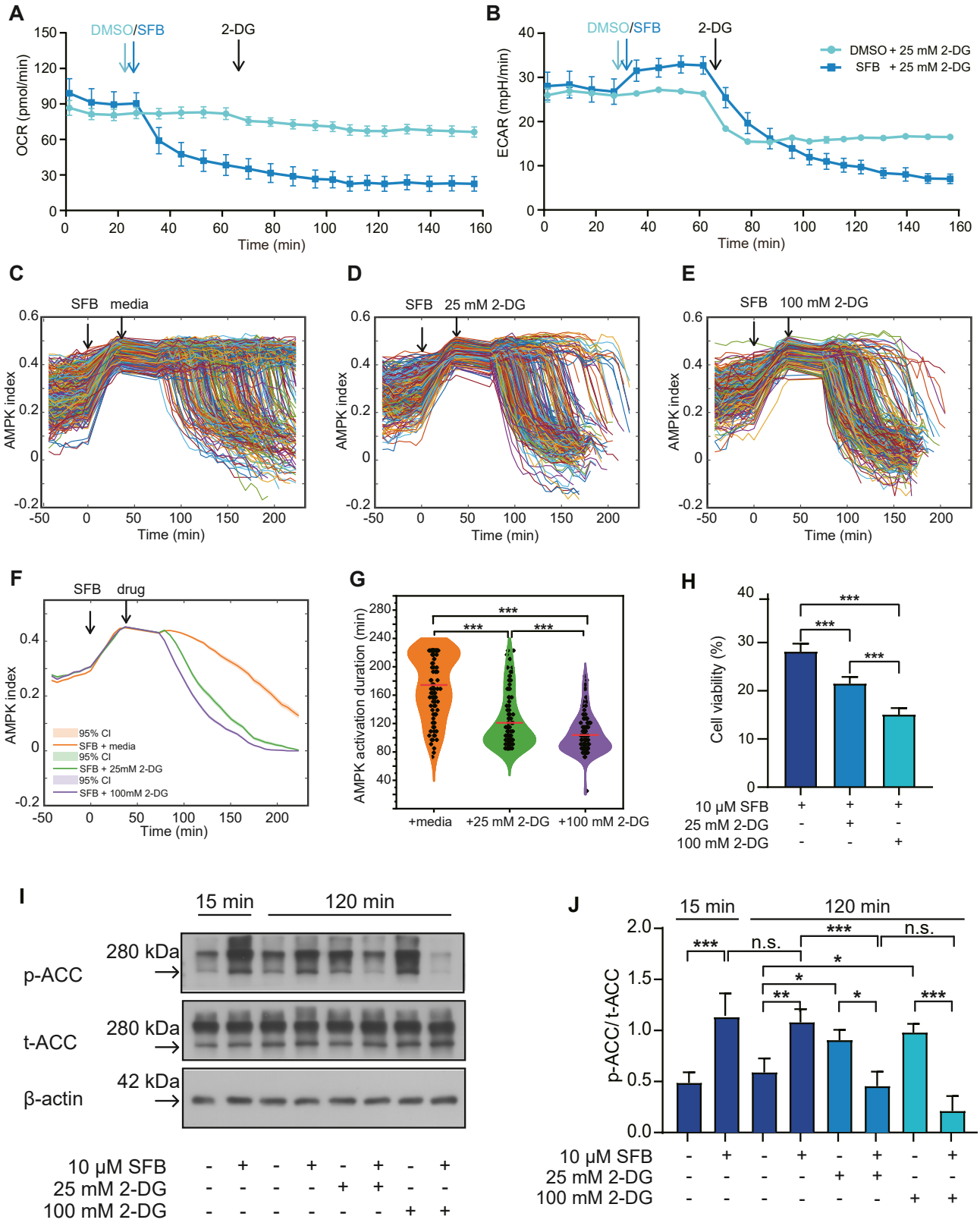

Figure 2: Glycolysis is necessary for sustained AMPK activation in response to sorafenib. (A) Oxygen consumption rate measured for cells treated with either DMSO or sorafenib (10 μM) and with 2-DG (25 mM) sequentially in high glucose. (B) Extracellular acidification rate measured for cells treated with the same conditions as in (A). (C–E) Single cell traces of AMPK index measured for cells cultured in 25 mM glucose with SFB (10 μM) added at time 0 and 2DG (0, 25 or 100 mM) at about 30 min later. (F) Mean and 95% confidence interval for traces of AMPK index from (C–E). (G) Activation duration of AMPK under the same treatments as in (F). (H) Cell viability of Huh7-AMPKAR2 in response to sorafenib alone or its combination with 2DG. (I) Western blots of ACC phosphorylation at different time points after sorafenib and 2DG treatment. Data representative of three independent experiments. (J) Quantification of ACC phosphorylation in (I). ***$p < 0.001$, **<0.01, *$p < 0.05$.

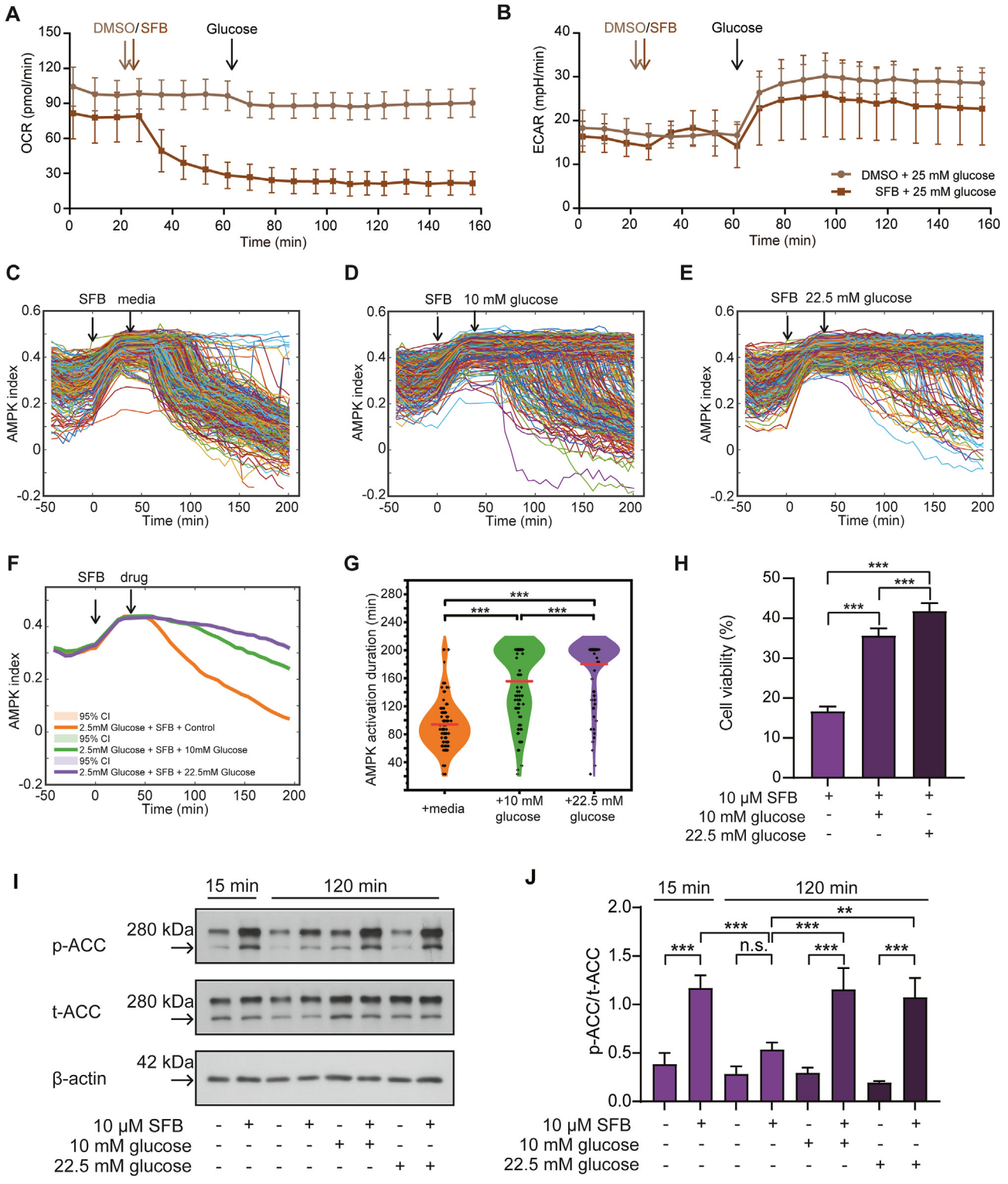

Figure 3: Glycolysis is sufficient for sustained AMPK activation in response to sorafenib. (A) Oxygen consumption rate measured for cells treated with either DMSO or sorafenib (10 μM) and with glucose (25 mM) sequentially in low glucose (2.5 mM). (B) Extracellular acidification rate measured for cells treated with the same conditions as in (A). (C–E) Single cell traces of AMPK index measured for cells cultured in 2.5 mM glucose with sorafenib added at time 0 and glucose (0, 12.5 or 25 mM) at about 30 min later. (F) Mean and 95% confidence interval for traces of AMPK index from (C–E). (G) Activation duration of AMPK under the same treatments as in (F). (H) Cell viability of Huh7-AMPKAR2 in response to sorafenib alone or its combination with glucose. (I) Western blots of ACC phosphorylation at different time points after sorafenib and glucose treatment. Data representative of three independent experiments. (J) Quantification of ACC phosphorylation in (I). ***$p < 0.001$, **<0.01, *$p < 0.05$.

increased by glucose supplementation after sorafenib treatment compared with sorafenib alone, indicating an increased or maintained AMPK activation with the drug combination (Figure 3I,J). In contrary, ACC phosphorylation was maintained or slightly decreased by glucose supplementation after DMSO compared with DMSO alone (Figure 3I). The results of western blot experiments were consistent with those of the FRET experiments. Glucose in combination with sorafenib also increased cell viability (Figure 3H), indicating the crucial role of glycolysis in maintaining viability in response to sorafenib. To study whether the promotion of AMPK activity by glycolysis in sorafenib pre-treatment is caused by adenine nucleotide ratios, we measured the levels of AMP, ADP and ATP in these treatments. The AMP to ATP ratio was decreased in the sorafenib + glucose condition, compared with sorafenib alone, which would cause a decrease in the AMPK activity (Figure. S5N-S5P and S7A). However, we observed that glucose supplementation increased the AMPK activity in single cells under sorafenib treatment, so this is not due to the changes in AMP/ATP.

4. DISCUSSION

Aerobic glycolysis or "Warburg effect" is a general and essential mechanism for cancer cells to evade mitochondrial inhibition under normoxia, or just a preferred route over oxidative phosphorylation to obtain ATP. It is regulated by many signaling pathways, including AMPK, PI3K/AKT, HIF-1α, c-Myc and a number of noncoding RNAs [20]. Since AMPK is very sensitive to changes in AMP/ATP ratio upon mitochondrial inhibition, it is activated and promotes glycolysis as an adaptive mechanism for HCC survival in response to sorafenib. Consistent with previous findings [25,29–32], high dose of sorafenib induces full AMPK activation within 15 min of treatment. By monitoring AMPK activity in real time in living cells, we find that the activation of AMPK induced by sorafenib is transient and its activation duration is prolonged with the increase of glucose concentration. Longer activation of AMPK, rather than higher levels of activation, correlates with better survival of HCCs in response to sorafenib in high glucose. Increasing glycolysis extends AMPK activation, whereas inhibiting glycolysis shortens it. It is well accepted that AMPK activates glycolysis which in turn inhibits AMPK activity through restoring energy levels. However, in sorafenib treatment, the regulation of glycolysis on AMPK was reversed such that glycolysis maintains AMPK activation. This regulation was not mediated by the AMP/ATP ratio, and warrants further exploration. Our findings suggest that glycolysis promotes sorafenib resistance through maintaining AMPK activation.

The role of AMPK in tumorigenesis and metastasis is still under debate. As a downstream target of the tumor suppressor gene LKB1, AMPK is thought to suppress tumor initiation. AMPKα knockout mice have an increased occurrence of Myc-drive lymphoma [33]. AMPK inhibits multiple cell growth pathways and promotes cell cycle arrest [19]. Due to its inhibitory role in tumor development, many AMPK activators (including metformin, phenformin or salicylates) are in clinical testing for treating multiple types of cancer. However, activating AMPK may be undesirable for established cancer in certain contexts, as this kinase aids cell survival under energetic stresses. AMPK-induced glycolysis is an important acquired resistance for a number of cancers under hypoxia [20]. AMPK also promotes tolerance to Ras inhibition by stimulating autophagy [34]. Therefore, effects of AMPK should be considered carefully based on tumor stage, tumor type and microenvironment. In the context of sorafenib-treated HCCs, accumulating evidence support that increasing glycolysis is an adaptive mechanism and AMPK is essential in this adaptation [20,25]. However, AMPK can either promote [20,35–37] or inhibit [38–42] glycolysis depending on the contexts; this discrepancy could be due to temporal dynamics of AMPK activity, selective regulation of AMPK on downstream targets, the crosstalk between AMPK with other glycolysis regulators, or the heterogeneous drug sensitivity in single cells. In terms of temporal regulation, short-term activation of AMPK increases glucose uptake and lactate production, but long-term activation of AMPK inhibits mTORC1 and hinders glucose metabolism in breast cancer cells treated with sorafenib [31]. Although it remains to be verified whether this mechanism is applicable to HCCs, it indicates that different durations of AMPK activation may regulate different pathways to control cancer proliferation, apoptosis, resistance and therapeutic effects. Our study is not enough to resolve the controversial role of AMPK in cancer development, but supports that AMPK is essential for maintaining cell survival in HCC resistance to sorafenib and that activation duration of AMPK may play an important role in drug resistance.

AMPKAR has recently been applied to study heterogeneity of cancer metabolism. A study monitored the real-time activity of AMPK in response to multiple oxidative phosphorylation inhibitors and showed that there were subclones resistant to AMPK activation induced by the inhibitors in multiple cancer cell types [43]. This insensitivity involves a combination of factors such as increased glucose uptake, decreased protein biosynthesis, and G0/G1 cell cycle arrest. This state can last for at least several hours and can be inherited during cell division. Similar intercellular metabolic heterogeneity was observed in our study (AMPK activity was heterogenerous among cells in response to sorafenib in high glucose), but we did not observe resistant subclones at the early time points. Sorafenib, as an inhibitor of mitochondrial respiration, induced AMPK activation in almost all Huh7 cells in the initial 15 min. We focused more on the total activation duration of AMPK and found that the duration of AMPK activation was negatively correlated with the sensitivity of HCC cells to sorafenib. It suggests that HCCs may be divided into subclones according to AMPK activation duration. To elucidate the molecular determinants of activation duration and drug sensitivity, we ought to profile the cells using the multi-omics approach or engineer the cells to express other biosensors which simultaneously monitor glycolysis, adenosine levels, cell cycle stage and so on.

Current study is limited in that it only studied AMPK dynamics in a single HCC cell line in response to one drug over a short period of time, it remains unclear whether the duration of AMPK activation is important in different cancer types, drugs or with longer treatment. Also, it is unclear whether AMPK dynamics is important *in vivo*. To study this, we should use xenograft models with Huh7-AMPKAR2 cells or transgenic mice expressing AMPKAR2. It remains to be tested whether therapeutic effects of sorafenib is modulated by AMPK dynamics in other solid tumors. This study shows that the AMP to ATP ratio was not the reason for sustained AMPK activation in response to sorafenib and high glucose, but has yet to find the factor downstream of glycolysis that activates AMPK. Since Huh7 cells express both LKB1 and CaMKK2 [44], these kinases may regulate AMPK activities. It could be that glycolysis regulates signaling pathways that are linked with LKB1 or CaMKK2 to regulate AMPK activity, or it acts through reactive oxygen species or the ubiquitin-based degradation to regulate AMPK. As cell morphology before cell death induced by sorafenib were different in different glucose, this suggests different modes of deaths in response to sorafenib in different glucose. Sorafenib can induce both ferroptosis [45] and apoptosis. AMPK induced by energy stress inhibits ferroptosis [46] and AMPK is activated by no glucose, so the cell death induced by sorafenib in no glucose is unlikely to be ferroptosis. But the exact modes of death in different glucose concentration and whether this plays a role in drug resistance need further clarification.

In summary, we provide the first evidence that glycolysis extends activation duration of AMPK during Warburg effect induced by sorafenib. This temporal regulation represents a new dimension where AMPK can reprogram metabolism and is an inherent property of AMPK regulation that has been neglected. Method of quantifying AMPK dynamics in both high-throughput and single-cell formats in response to therapeutics developed in this paper can be easily applied to other AMPK activators or inhibitors, or to study roles of AMPK in other cancer or metabolic diseases.

DECLARATION OF COMPETING INTEREST

This study was supported by the National Natural Science Foundation of China (Grant No. 881973403, 81841003), Peking University Seed Fund for Medicine-Information Interdisciplinary Research Project (Grant No. BMU2020MI004), Peking University Health Science Center Start-up Project (Grant No. BMU2018YJ012, BMU2021YJ053). We are deeply grateful to Professor John Albeck from University of California Davis to share with us the AMPKAR2 plasmid. We thank Dr. Han Xiao from the Third hospital of Peking University for many fruitful discussions and thoughtful advice. We thank Dr. Jia-Ren Lin from Laboratory of Systems Pharmacology at Harvard Medical School for great suggestions in Image analysis and deposition. We thank Yiming Wang and Songmin Liu for being nice colleagues and help in the lab. We thank Megarobo Inc. (Beijing, China) for their support in high-content fluorescence microscope imaging. We thank the Facility Center of Metabolomics and Lipidomics of China National Center for Protein Sciences (Tsinghua University) for the metabolomics profiling. There is no conflict of interest to declare for any author.

DATA AVAILABILITY

Data will be made available on request.

ACKNOWLEDGEMENT

This study was supported by the National Natural Science Foundation of China (Grant No. 881973403, 81841003), Peking University Seed Fund for Medicine-Information Interdisciplinary Research Project (Grant No. BMU2020MI004), Peking University Health Science Center Start-up Project (Grant No. BMU2018YJ012, BMU2021YJ053). We are deeply grateful to Professor John Albeck from University of California Davis to share with us the AMPKAR2 plasmid. We thank Dr. Han Xiao from the Third hospital of Peking University for many fruitful discussions and thoughtful advice. We thank Dr. Jia-Ren Lin from Laboratory of Systems Pharmacology at Harvard Medical School for great suggestions in Image analysis and deposition. We thank Lina Wang and Xinyu Zhou for western blotting experiments during paper revision. We thank Megarobo Inc. (Beijing, China) for their support in high-content fluorescence microscope imaging. We thank the Facility Center of Metabolomics and Lipidomics of China National Center for Protein Sciences (Tsinghua University) for the metabolomics profiling. There is no conflict of interest to declare for any author.

APPENDIX A. SUPPLEMENTARY DATA

Supplementary data to this article can be found online at https://doi.org/10.1016/j.molmet.2023.101796.

REFERENCES

[1] Garcia D, Shaw RJ. AMPK: mechanisms of cellular energy sensing and restoration of metabolic balance. Mol Cell 2017;66:789–800.

[2] Lin S-C, Hardie DG. AMPK: sensing glucose as well as cellular energy status. Cell Metabol 2018;27:299–313.

[3] Zhang C-S, Hawley SA, Zong Y, Li M, Wang Z, Gray A, et al. Fructose-1,6-bisphosphate and aldolase mediate glucose sensing by AMPK. Nature 2017;548:112–6.

[4] Hawley SA, Pan DA, Mustard KJ, Ross L, Bain J, Edelman AM, et al. Calmodulin-dependent protein kinase kinase-beta is an alternative upstream kinase for AMP-activated protein kinase. Cell Metabol 2005;2:9–19.

[5] Woods A, Dickerson K, Heath R, Hong S-P, Momcilovic M, Johnstone SR, et al. Ca2+/calmodulin-dependent protein kinase kinase-beta acts upstream of AMP-activated protein kinase in mammalian cells. Cell Metabol 2005;2:21–33.

[6] Hurley RL, Anderson KA, Franzone JM, Kemp BE, Means AR, Witters LA. The Ca2+/calmodulin-dependent protein kinase kinases are AMP-activated protein kinase kinases. J Biol Chem 2005;280:29060–6.

[7] Trefts E, Shaw RJ. AMPK: restoring metabolic homeostasis over space and time. Mol Cell 2021;81:3677–90.

[8] Zhang C-S, Jiang B, Li M, Zhu M, Peng Y, Zhang Y-L, et al. The lysosomal v-ATPase-Ragulator complex is a common activator for AMPK and mTORC1, acting as a switch between catabolism and anabolism. Cell Metabol 2014;20:526–40.

[9] Zong Y, Zhang C-S, Li M, Wang W, Wang Z, Hawley SA, et al. Hierarchical activation of compartmentalized pools of AMPK depends on severity of nutrient or energy stress. Cell Res 2019;29:460–73.

[10] Cao Y, Bojjireddy N, Kim M, Li T, Zhai P, Nagarajan N, et al. Activation of γ2-AMPK suppresses ribosome biogenesis and protects against myocardial ischemia/reperfusion injury. Circ Res 2017;121:1182–91.

[11] Chen X, Li X, Zhang W, He J, Xu B, Lei B, et al. Activation of AMPK inhibits inflammatory response during hypoxia and reoxygenation through modulating JNK-mediated NF-κB pathway. Metabolism 2018;83:256–70.

[12] Hung C-M, Lombardo PS, Malik N, Brun SN, Hellberg K, Van Nostrand JL, et al. AMPK/ULK1-mediated phosphorylation of Parkin ACT domain mediates an early step in mitophagy. Sci Adv 2021;7:eabg4544.

[13] Condon KJ, Orozco JM, Adelmann CH, Spinelli JB, van der Helm PW, Roberts JM, et al. Genome-wide CRISPR screens reveal multitiered mechanisms through which mTORC1 senses mitochondrial dysfunction. Proc Natl Acad Sci USA 2021;118:e2022120118.

[14] Tsou P, Zheng B, Hsu C-H, Sasaki AT, Cantley LC. A fluorescent reporter of AMPK activity and cellular energy stress. Cell Metabol 2011;13:476–86.

[15] Miyamoto T, Rho E, Sample V, Akano H, Magari M, Ueno T, et al. Compartmentalized AMPK signaling illuminated by genetically encoded molecular sensors and actuators. Cell Rep 2015;11:657–70.

[16] Schmitt DL, Rho E, Sample V, Akano H, Magari M, Ueno T, et al. Spatial regulation of AMPK signaling revealed by a sensitive kinase activity reporter. Nat Commun 2022;13:1–12.

[17] Hung YP, Teragawa C, Kosaisawe N, Gillies TE, Pargett M, Minguet M, et al. Akt regulation of glycolysis mediates bioenergetic stability in epithelial cells. Elife 2017;6:e27293.

[18] Konagaya Y, Terai K, Hirao Y, Takakura K, Imajo M, Kamioka Y, et al. A highly sensitive FRET biosensor for AMPK exhibits heterogeneous AMPK responses among cells and organs. Cell Rep 2017;21:2628–38.

[19] Steinberg GR, Carling D. AMP-activated protein kinase: the current landscape for drug development. Nat Rev Drug Discov 2019;18:527–51.

[20] Feng J, Li J, Wu L, Yu Q, Ji J, Wu J, et al. Emerging roles and the regulation of aerobic glycolysis in hepatocellular carcinoma. J Exp Clin Cancer Res 2020;39:126.

[21] Reyes R, Wani NA, Ghoshal K, Jacob ST, Motiwala T. Sorafenib and 2-deoxyglucose synergistically inhibit proliferation of both sorafenib sensitive and resistant HCC cells by inhibiting ATP production. Gene Expr 2017;17:129–40.

[22] Li S, Dai W, Mo W, Li J, Feng J, Wu L, et al. By inhibiting PFKFB3, aspirin overcomes sorafenib resistance in hepatocellular carcinoma. Int J Cancer 2017;141:2571–84.

[23] Shen Y-C, Ou D-L, Hsu C, Lin K-L, Chang C-Y, Lin C-Y, et al. Activating oxidative phosphorylation by a pyruvate dehydrogenase kinase inhibitor overcomes sorafenib resistance of hepatocellular carcinoma. Br J Cancer 2013;108:72–81.
[24] Krstic J, Reinisch I, Schindlmaier K, Galhuber M, Riahi Z, Berger N, et al. Fasting improves therapeutic response in hepatocellular carcinoma through p53-dependent metabolic synergism. Sci Adv 2022;8:eabh2635.
[25] Tesori V, Piscaglia AC, Samengo D, Barba M, Bernardini C, Scatena R, et al. The multikinase inhibitor Sorafenib enhances glycolysis and synergizes with glycolysis blockade for cancer cell killing. Sci Rep 2015;5:9149.
[26] Maximchik P, Abdrakhmanov A, Inozemtseva E, Tyurin-Kuzmin PA, Zhivotovsky B, Gogvadze V. 2-Deoxy-D-glucose has distinct and cell line-specific effects on the survival of different cancer cells upon antitumor drug treatment. FEBS J 2018;285:4590–601.
[27] Zhang J, Dong Y, Xu Z, Zhang Y, Pan C, McAuliffe S, et al. 2-Deoxy-D-glucose attenuates isoflurane-induced cytotoxicity in an in vitro cell culture model of H4 human neuroglioma cells. Anesth Analg 2011;113:1468–75.
[28] Clem B, Telang S, Clem A, Yalcin A, Meier J, Simmons A, et al. Small-molecule inhibition of 6-phosphofructo-2-kinase activity suppresses glycolytic flux and tumor growth. Mol Cancer Therapeut 2008;7:110–20.
[29] Jian C, Fu J, Cheng X, Shen L-J, Ji Y-X, Wang X, et al. Low-dose sorafenib acts as a mitochondrial uncoupler and ameliorates nonalcoholic steatohepatitis. Cell Metabol 2020;31:892–908.e11.
[30] Ross FA, Hawley SA, Auciello FR, Gowans GJ, Atrih A, Lamont DJ, et al. Mechanisms of paradoxical activation of AMPK by the kinase inhibitors SU6656 and sorafenib. Cell Chem Biol 2017;24:813–824.e4.
[31] Fumarola C, Hawley SA, Auciello FR, Gowans GJ, Atrih A, Lamont DJ, et al. Effects of sorafenib on energy metabolism in breast cancer cells: role of AMPK–mTORC1 signaling. Breast Cancer Res Treat 2013;141:67–78.
[32] Groenendijk FH, Mellema WW, van der Burg E, Schut E, Hauptmann M, Horlings HM, et al. Sorafenib synergizes with metformin in NSCLC through AMPK pathway activation. Int J Cancer 2015;136:1434–44.
[33] Faubert B, Boily G, Izreig S, Griss T, Samborska B, Dong Z, et al. AMPK is a negative regulator of the Warburg Effect and suppresses tumor growth in vivo. Cell Metabol 2013;17:113–24.
[34] Sanduja S, Feng Y, Mathis RA, Sokol ES, Reinhardt F, Halaban R, et al. AMPK promotes tolerance to Ras pathway inhibition by activating autophagy. Oncogene 2016;35:5295–303.
[35] Hardie DG. AMPK: a target for drugs and natural products with effects on both diabetes and cancer. Diabetes 2013;62:2164–72.
[36] Wu N, Zheng B, Shaywitz A, Dagon Y, Tower C, Bellinger G, et al. AMPK-dependent degradation of TXNIP upon energy stress leads to enhanced glucose uptake via GLUT1. Mol Cell 2013;49:1167–75.
[37] Marsin A-S, Bertrand L, Rider MH, Deprez J, Beauloye C, Vincent MF, et al. Phosphorylation and activation of heart PFK-2 by AMPK has a role in the stimulation of glycolysis during ischaemia. Curr Biol 2000;10:1247–55.
[38] Ren Y, Bertrand L, Rider MH, Deprez J, Beauloye C, Vincent MF, et al. CXCR3 confers sorafenib resistance of HCC cells through regulating metabolic alteration and AMPK pathway. Am J Transl Res 2020;12:825–36.
[39] Bi L, Ren Y, Feng M, Meng P, Wang Q, Chen W, et al. HDAC11 regulates glycolysis through the LKB1/AMPK signaling pathway to maintain hepatocellular carcinoma stemness. Cancer Res 2021;81:2015–28.
[40] Fang G, Zhang P, Liu J, Zhang X, Zhu X, Li R, et al. Inhibition of GSK-3β activity suppresses HCC malignant phenotype by inhibiting glycolysis via activating AMPK/mTOR signaling. Cancer Lett 2019;463:11–26.
[41] Hu L, Zeng Z, Xia Q, Liu Z, Feng X, Chen J, et al. Metformin attenuates hepatoma cell proliferation by decreasing glycolytic flux through the HIF-1α/PFKFB3/PFK1 pathway. Life Sci 2019;239:116966.
[42] Tseng H-I, Zeng Y-S, Lin Y-CJ, Huang J-W, Lin C-L, Lee M-H, et al. A novel AMPK activator shows therapeutic potential in hepatocellular carcinoma by suppressing HIF1α-mediated aerobic glycolysis. Mol Oncol 2022;16:2274–94.
[43] Kosaisawe N, Sparta B, Pargett M, Teragawa CK, Albeck JG. Transient phases of OXPHOS inhibitor resistance reveal underlying metabolic heterogeneity in single cells. Cell Metabol 2021;33:649–665.e8.
[44] Zhang J, Wang E, Zhang L, Zhou B. PSPH induces cell autophagy and promotes cell proliferation and invasion in the hepatocellular carcinoma cell line Huh7 via the AMPK/mTOR/ULK1 signaling pathway. Cell Biol Int 2021;45:305–19.
[45] Dixon SJ, Patel DN, Welsch M, Skouta R, Lee ED, Hayano M, et al. Pharmacological inhibition of cystine–glutamate exchange induces endoplasmic reticulum stress and ferroptosis. Elife 2014;3.
[46] Lee H, Zandkarimi F, Zhang Y, Meena JK, Kim J, Zhuang L, et al. Energy-stress-mediated AMPK activation inhibits ferroptosis. Nat Cell Biol 2020;22:225–34.

